The crystal structure and electronic properties of a new metastable non-stoichiometric $BaAl_4$-type compound crystallized from amorphous $La_6Ni_{34}Ge_{60}$ alloy

2004 J. Phys.: Condens. Matter 16 7917

(http://iopscience.iop.org/0953-8984/16/45/014)

INSTITUTE OF PHYSICS PUBLISHING JOURNAL OF PHYSICS: CONDENSED MATTER

J. Phys.: Condens. Matter **16** (2004) 7917–7930 PII: S0953-8984(04)84358-3

The crystal structure and electronic properties of a new metastable non-stoichiometric $BaAl_4$-type compound crystallized from amorphous $La_6Ni_{34}Ge_{60}$ alloy

Masashi Hasegawa[1], Shoichiro Suzuki[1], Tetsu Ohsuna[1], Eiichiro Matsubara[1], Satoshi Endo[2] and Akihisa Inoue[1]

[1] Institute for Materials Research, Tohoku University, Sendai, Katahira 980-8577, Japan
[2] Center for Low Temperature Science, Tohoku University, Sendai, Katahira 980-8577, Japan

Received 28 July 2004, in final form 10 September 2004
Published 29 October 2004
Online at stacks.iop.org/JPhysCM/16/7917
doi:10.1088/0953-8984/16/45/014

Abstract

A new metastable La–Ge–Ni ternary $BaAl_4$-type ($ThCr_2Si_2$-type) compound, of which the space group is $I4/mmm$ is synthesized. It is obtained by a polymorphic transformation from an $La_6Ni_{34}Ge_{60}$ amorphous alloy on crystallizing. The formula of the compound is $(La_{0.3}Ge_{0.7})(Ni_{0.85}Ge_{0.15})_2Ge_2$. This indicates that it is highly non-stoichiometric compared to the stoichiometric $LaNi_2Ge_2$. It is found that the c-axis lattice parameter of this compound is much longer than that of $LaNi_2Ge_2$. It should be noted that the longer c-axis unit cell parameter is attributable only to the longer interlayer distance between Ge site and Ni site layers. The temperature dependences of electrical resistivity and thermoelectric power of the $(La_{0.3}Ge_{0.7})(Ni_{0.85}Ge_{0.15})_2Ge_2$ compound and $La_6Ni_{34}Ge_{60}$ amorphous alloy are also clarified. The comparison of these electronic properties between the two materials indicates that sp-electrons mainly contribute to the density of states around the Fermi level of this compound.

1. Introduction

The crystallization behaviour of amorphous alloys has mainly been investigated from the viewpoint of local structure and thermal stability of amorphous alloys by many researchers. However, the crystallization behaviour is also interesting from the viewpoint of obtaining a new compound. The crystallization of an amorphous alloy is usually multistage, and sometimes produces metastable compounds before the completely stable final stage in the crystallization process. The metastable compounds are interesting because they might be new compounds with a new crystal structure. In particular, the polymorphic transformation from an amorphous phase to a metastable crystalline one on crystallizing is most interesting because the crystallized

alloy is of only single phase, and so it is easier to investigate the crystal structure and crystal chemistry of a new metastable compound compared to a multiphase crystallized alloy.

A polymorphic transformation of an amorphous alloy to a metastable compound has been sometimes reported. For example, Imafuku *et al* reported recently a polymorphic transformation of an amorphous alloy in the Fe–Nb–B system [1]. They reported polymorphic transformations from an amorphous phase to an α-Mn-type compound on crystallizing and then to an α-Fe-type one in an $Fe_{60}Nb_{10}B_{30}$ alloy. In addition, $Fe_{80}Nb_{10}B_{10}$ was also reported to show a polymorphic transformation from an amorphous phase to an $Fe_{23}B_6$-type compound on crystallizing. Although they investigated only from the viewpoint of local structure and stability of the amorphous alloys, these were new metastable compounds having interesting structure.

In this paper the crystallization behaviours of $La_6Ni_{34}Ge_{60}$ amorphous alloys and crystallized metastable compound are described from the viewpoint of crystal structure at first because Louzguine *et al* suggested a possibility of a polymorphic transformation on crystallizing the Ge-rich amorphous $La_5Ni_{33}Ge_{60}$ alloy [2]. Then, the temperature dependences of thermoelectric power and electrical resistivity of the metastable crystalline and amorphous phases are also shown and discussed from the viewpoints of the electronic structure and phase stability of the metastable compound.

2. Experimental procedure

Mother ingots of $La_5Ni_{33}Ge_{60}$ alloys were prepared by arc melting of a mixture of pure metals La (99.9%), Ni (99.99%) and Ge (99.999%) in an argon atmosphere purified using a Ti getter. Alloy ribbons were prepared by a single-roller melt spinning technique in an argon atmosphere. The composition of the ribbons was inspected by a scanning electron microscope with an energy dispersive x-ray spectroscopy (SEM-EDX). The inspected composition was $La_{6.0}Ni_{34.2}Ge_{59.8}$. This is almost the same as the nominal composition. This inspected composition $La_6Ni_{34}Ge_{60}$ is used as the sample composition in this paper.

Thermal stability and phase transformation were investigated by a differential scanning calorimeter (DSC) at a heating rate of 0.67 K s^{-1} in a purified argon atmosphere. Isothermal annealing of samples was also carried out for 10 min in the DSC apparatus in a purified argon atmosphere on the basis of the DSC results. The crystal structures were investigated by transmission electron microscopy (TEM) and ordinary x-ray powder diffractometry using Cu Kα radiation with an Ni filter. Thin samples for transmission electron microscopy observations were prepared by dimpling and ion-milling carefully. Before grinding a small ribbon of about 20 μm in thickness was cut and polished with sandpapers. Both sides of the ribbon were ground and polished to 15 μm, dimpled to 10 μm and then finally thinned by ion-milling. The TEM investigation was carried out by using a JEM-4000EX microscope operating at 400 kV and equipped with EDX. The x-ray powder diffraction data were analysed by Rietveld analysis using the RIETAN-2000 program [3].

The temperature dependence of the DC electrical resistivity was measured by a conventional four-probe method between 4.2 and 300 K. The temperature dependence of the thermoelectric power was measured by a conventional DC method between 80 and 400 K. The temperature difference to measure the thermoelectric power was about 5 K. The thermoelectric power was measured three times at each temperature and then the averaged value was used for the datum.

3. Results and discussion

3.1. Crystallization process

Figure 1 shows an x-ray scattering intensity profile of as-spun alloy. No diffraction peaks are observed in the profile, indicating an amorphous structure. Figure 2 shows a DSC curve.

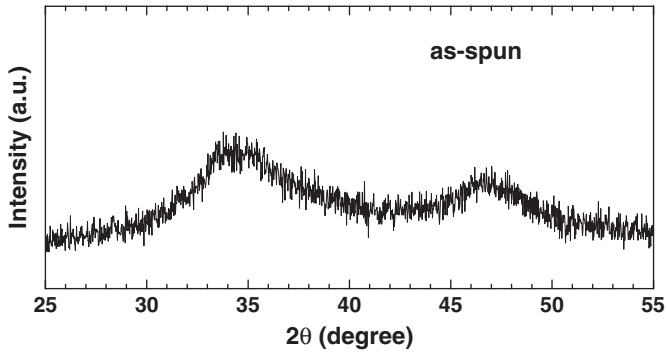

Figure 1. X-ray scattering intensity profile of as-spun $La_6Ni_{34}Ge_{60}$ alloy.

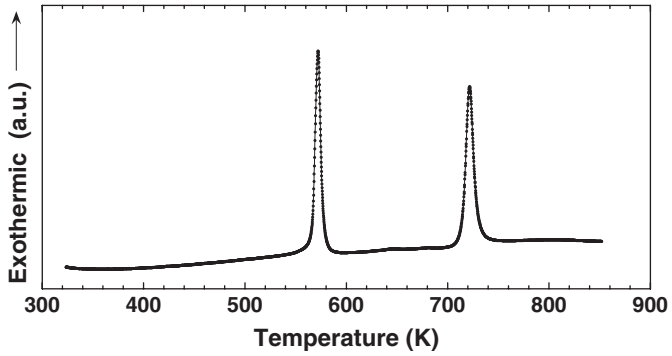

Figure 2. DSC curve of as-spun $La_6Ni_{34}Ge_{60}$ alloy.

There is the first sharp exothermic peak at 577 K. This may correspond to a crystallization. Figure 3 shows x-ray powder diffraction patterns of the annealed samples. One is of the sample annealed at about 580 K, which is above the first peak in the DSC curve in figure 2. The other is of the sample annealed at about 800 K, which is above the second peak in the DSC curve in figure 2. It is found that many sharp diffraction peaks can be observed in the diffraction pattern of the former sample. This indicates that the first peak of the DSC curve exactly corresponds to the crystallization. It is also found that the former pattern is different from the latter one. In addition, the latter one can be identified by the three stable compounds $LaNi_2Ge_2$, Ge and GeNi, as shown in figure 3. These results mean that the state between the first and second peaks is metastable in the crystallization process of amorphous $La_6Ni_{34}Ge_{60}$.

Figure 4 shows a TEM image of the metastable $La_6Ni_{34}Ge_{60}$. Grains with size from several tens of nanometres to several hundreds of nanometres are observed, and no amorphous phase is observed at the grain boundary. The EDX inspections of several single grains showed that the composition of each single grain was the same: $La_{6.0}Ni_{34.3}Ge_{59.7}$. This composition is also the same as the composition determined by the SEM ($La_{6.0}Ni_{34.2}Ge_{59.8}$) mentioned in the previous section. These results indicate that the metastable crystallized alloy is composed of a single phase. Accordingly, the crystallization of amorphous $La_6Ni_{34}Ge_{60}$ alloy is clearly a polymorphic transformation from an amorphous to a metastable crystalline phase.

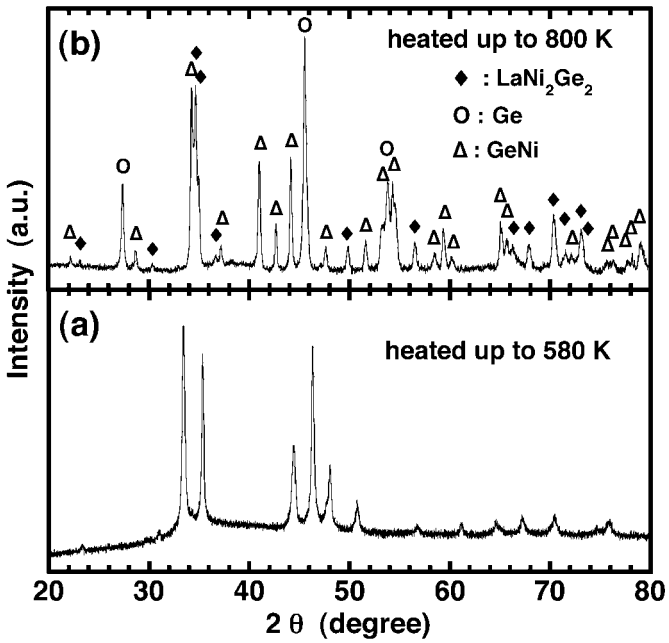

Figure 3. X-ray powder diffraction pattern of $La_6Ni_{34}Ge_{60}$ after being heated up to about 580 and 800 K, which are above the first and second sharp peak in the DSC curve in figure 2, respectively. (a) Heated up to 580 K, (b) heated up to 800 K.

3.2. Identification and crystal structure of the metastable compound

Since the crystallized sample was found to be of a single metastable phase, as mentioned above, the phase search application program was used to identify the x-ray diffraction pattern of the metastable phase. Fortunately, some trials lead to one good coincidence, i.e. with the pattern[3] of $SrCo_2Ge_2$, as shown below the x-ray pattern in figure 5. $SrCo_2Ge_2$ has a tetragonal crystal structure with lattice parameters $a = 4.08(1)$ Å, $c = 10.65(2)$ Å, respectively [4]. Since the x-ray diffraction scattering angles are almost the same as those of $SrCo_2Ge_2$, it is found that the crystal structure of the $La_6Ni_{34}Ge_{60}$ metastable phase is tetragonal and that the lattice parameters are almost the same as those of $SrCo_2Ge_2$. In order to investigate the details of the crystal structure of the metastable phase, TEM diffraction patterns were also taken in various directions, such as [100], [110], [001], [201] and [531]. For example, figure 6 shows diffraction patterns of the case of the incident beam parallel to the [001] directions. It was found that all diffractions patterns in each direction were identified to be of a tetragonal structure. In addition, it was also found that the reflection condition completely satisfied $h + k + l = 2n$ (even). This indicates that the $La_6Ni_{34}Ge_{60}$ metastable phase is of a body-centred lattice structure. It is concluded from these results that the metastable $La_6Ni_{34}Ge_{60}$ phase in this study has a unit cell of the body-centred tetragonal crystal structure.

$SrCo_2Ge_2$, of which the x-ray diffraction patterns are almost the same as that of the metastable compound, is an isostructure of $BaAl_4(ThCr_2Si_2)$, with symmetry $I4/mmm$ [4]. In addition, a stable stoichiometric compound $LaNi_2Ge_2$, which also has the isostructure of $BaAl_4$, was also reported in the La–Ge–Ni alloy system [5]. There is actually the stable stoichiometric compound $LaNi_2Ge_2$ in the x-ray diffraction pattern of the stable $La_6Ni_{34}Ge_{60}$

[3] JCPDF file 30–439.

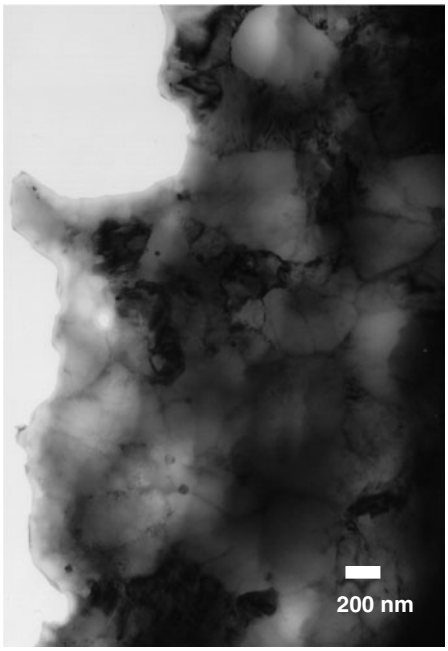

Figure 4. TEM image of the metastable $La_6Ni_{34}Ge_{60}$. The sample was prepared by annealing at 580 K, which is just above the first peak (crystallization peak) in the DSC curve in figure 2, for 10 min in the DSC apparatus.

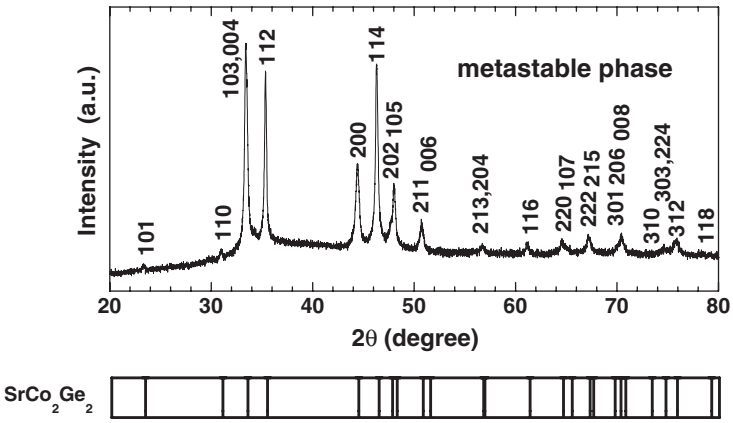

Figure 5. X-ray powder diffraction pattern of the metastable $La_6Ni_{34}Ge_{60}$ phase. The reflection degree positions of $SrCo_2Ge_2$ are also shown below the pattern.

alloy in this study, as shown in figure 3. These results strongly suggest that the metastable $La_6Ni_{34}Ge_{60}$ phase may also be a compound having the $BaAl_4$-type structure, although the composition of $La_6Ni_{34}Ge_{60}$ is considerably different from the stable $LaNi_2Ge_2$ ($La_{20}Ni_{40}Ge_{40}$) compound.

The $BaAl_4$-type structure is of a body-centred tetragonal unit cell ($I4/mmm$, no. 139), as shown in figure 7 [6, 7]. The Ba atoms occupy the corner and centre positions. The Al atoms are located in two independent sites. Al_a atoms in one site occupy the Wyckoff site 4d

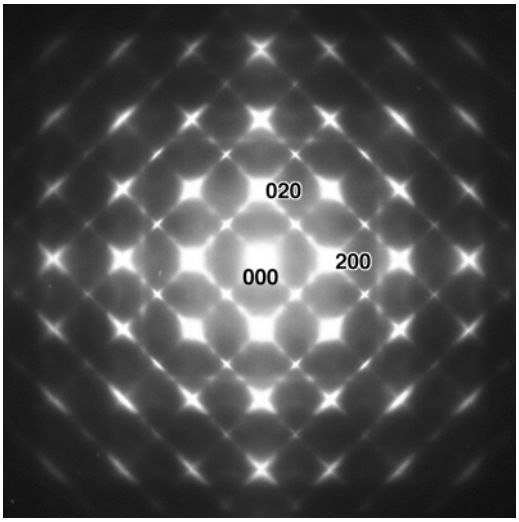

Figure 6. TEM diffraction patterns of the metastable $La_6Ni_{34}Ge_{60}$ phase. The incident beam is parallel to the [001] directions.

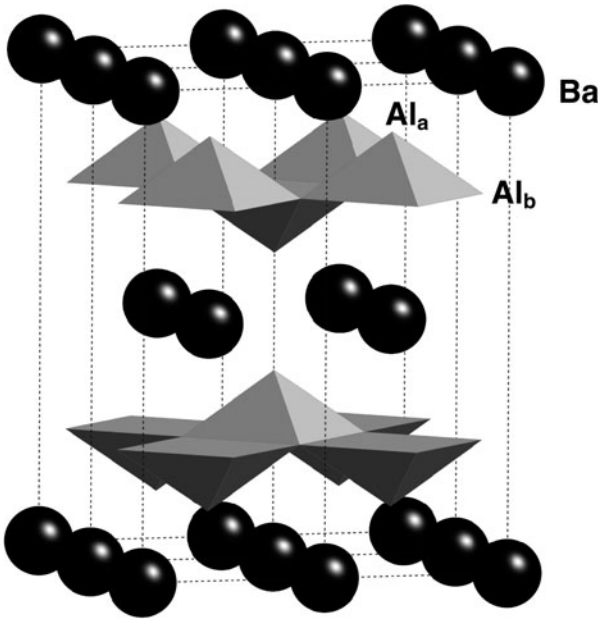

Figure 7. Crystal structure of the binary $BaAl_4$-type compounds.

(1/2, 0, 1/4) and form a two-dimensional square plane. Al_b atoms in the other site occupy the Wyckoff site 4e (0, 0, z). Thus, the Al atoms form Al_5-square pyramids above and below the two-dimensional square plane alternately. These are connected by the Al_b–Al_b bond in the two-dimensional square plane, as shown in figure 7. Since there are numbers of compounds having this structure [8, 9], a number of studies on the $BaAl_4$-type compounds have been reported, such as their crystal chemistry, magnetism, and so on [9–18].

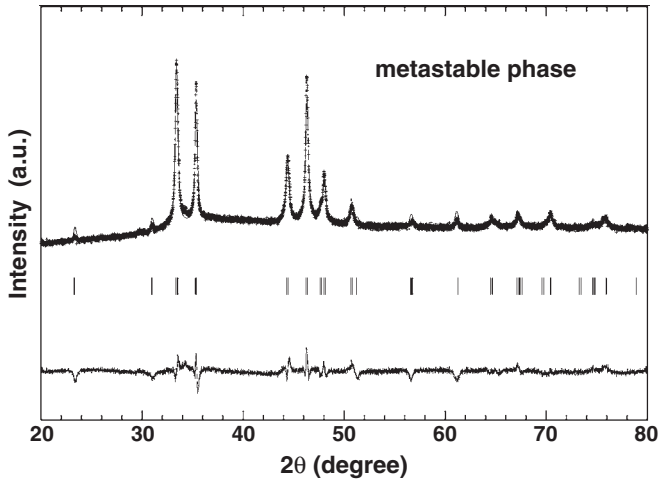

Figure 8. Fitting result of the x-ray diffraction pattern of $La_6Ni_{34}Ge_{60}$ by the Rietveld method.

In the case of the stoichiometric $LaNi_2Ge_2$, the Ni atoms are located in the 4e site (Al_a) and the Ge ones are in the 4d site (Al_b), respectively. These occupations are basically the same as the structure of the $ThCr_2Si_2$-type structure which is usually used for the ternary stoichiometric $BaAl_4$-type structure. The Ni atoms form a two-dimensional square plane, and then the Ni and Ge atoms form $GeNi_4$-square pyramids. Accordingly, each Ni atom is surrounded almost tetrahedrally by four Ge atoms, and each Ge atom is surrounded by four Ni atoms and one Ge atom at the apex of the $GeNi_4$-square pyramid. The La atoms, having large atomic radius, are located in the centre of this framework in which there is a large void.

As mentioned above, since there is a possibility that the metastable $La_6Ni_{34}Ge_{60}$ phase in this study is also a compound having the $BaAl_4$-type structure, the Rietveld analysis has been applied using a model of the $BaAl_4$-type structure. The analysed composition of the compound in this study is $La_6Ni_{34}Ge_{60}$, as mentioned above. This is much more Ge-rich than the stoichiometric $LaNi_2Ge_2$ ($La_{20}Ni_{40}Ge_{40}$). Accordingly, models containing vacancies at the La and/or Ni sites were, at first, tried for the Rietveld analysis. However, the x-ray diffraction data were not fitted. Then, another model of $(La_{0.3}Ge_{0.7})(Ni_{0.85}Ge_{0.15})_2Ge_2$ was tried. In this model there are no vacancies, and Ge atoms occupy both of the La and Ni sites at random. At first we selected one unique ideal atomic position of the (La, Ge) site for the Rietveld analysis. Although the x-ray diffraction data were almost fitted by this model, a very large atomic displacement parameter of this site was obtained. This may be attributable to the displacement of the atomic position of Ge atoms at the La site because of the much smaller atomic radius of the Ge atom (1.23 Å) than the La atom (1.88 Å). Accordingly, we displaced the position of the (La, Ge) site and refined the position again. In this case, the Wyckoff position of this site was changed from 2a to 16m and so the full occupancy was also changed from 1 to 0.125. Then, a better fitting result was obtained. The fitting result and the parameters are shown in figure 8 and tables 1 and 2. Figure 9 shows the refined crystal structure of $(La_{0.3}Ge_{0.7})(Ni_{0.85}Ge_{0.15})_2Ge_2$ in this study. The crystal structure of $LaNi_2Ge_2$ is also shown for comparison in figure 9. In order to reconfirm if this result is reasonable, high resolution TEM (HRTEM) images were also observed and compared to the simulated image of this model. Figure 10 shows an HRTEM image of the metastable compound with the incident beam parallel to the [100] direction, and the corresponding electron diffraction patterns and a

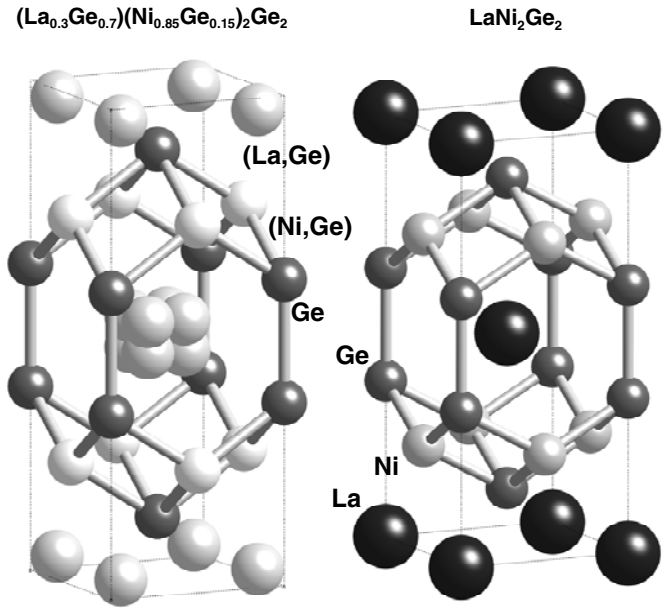

Figure 9. The crystal structure of $(La_{0.3}Ge_{0.7})(Ni_{0.85}Ge_{0.15})_2Ge_2$ and $LaNi_2Ge_2$. (La, Ge) and (Ni, Ge) means $(La_{0.3}Ge_{0.7})$ and $(Ni_{0.85}Ge_{0.15})$, respectively.

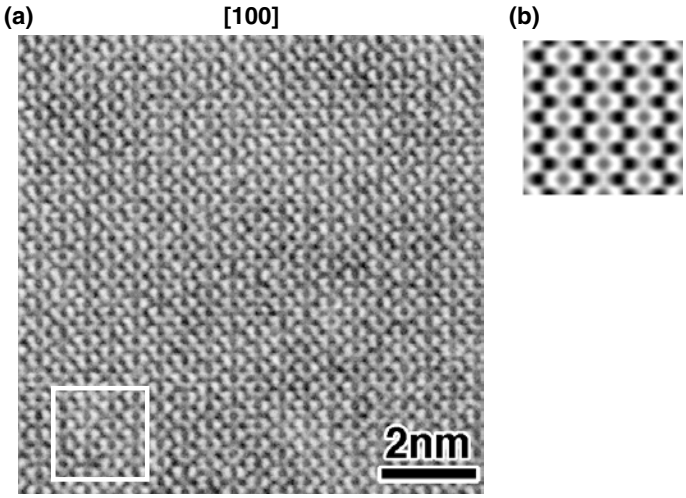

Figure 10. (a) High resolution TEM (HRTEM) images of the metastable $La_6Ni_{34}Ge_{60}$ phase. (b) Simulated images of the $BaAl_4$-type $(La_{0.3}Ge_{0.7})(Ni_{0.85}Ge_{0.15})_2Ge_2$.

simulated image of $(La_{0.3}Ge_{0.7})(Ni_{0.85}Ge_{0.15})_2Ge_2$ in which the parameters obtained from the Rietveld analysis above were used. It is found that the simulated image coincides well with the observed HRTEM images. This indicates that the metastable $La_6Ni_{34}Ge_{60}$ compound is of the $BaAl_4$-type having a formula of $(La_{0.3}Ge_{0.7})(Ni_{0.85}Ge_{0.15})_2Ge_2$. This means that it is an extremely non-stoichiometric compound compared to the stoichiometric one. Therefore, this is a new highly non-stoichiometric metastable $BaAl_4$-type compound in the Ge–Ni–La ternary

Table 1. Selected results of the Rietveld refinements for $La_6Ni_{34}Ge_{60}$.

Formula	$(La_{0.3}Ge_{0.7})(Ni_{0.85}Ge_{0.15})_2Ge_2$	Density (calc.)	$d = 6.712\,49$ g cm^{-3}
Crystal system	Tetragonal	Radiation	Cu Kα (Ni filter)
Space group	$I4/mmm$ (no. 139)	2θ	20°–80°
Z	2	R_p	0.0397
Lattice parameters	$a = 4.080\,10(15)$ Å	R_{wp}	0.0531
	$c = 10.677\,90(49)$ Å	R_e	0.0684
	$c/a = 2.617\,07$	R_I	0.0508
Volume	$V = 177.7573(122)$ Å^3	R_F	0.0256

Table 2. Atomic positional parameters for $(La_{0.3}Ge_{0.7})(Ni_{0.85}Ge_{0.15})_2Ge_2$.

Atom	Wyckoff position	x	y	z	Occ.
LaGe[a]	16m	0.104 76(72)	0.104 76(72)	0.031 66(38)	0.125
Ge	4e	0	0	0.374 51(15)	1
NiGe[a]	4d	0	1/2	1/4	1

[a] LaGe and NiGe mean $La_{0.3}Ge_{0.7}$ and $Ni_{0.85}Ge_{0.15}$, respectively.

system. Although there are numbers of compounds having the $BaAl_4$-type structure [8, 9], there are limited reports of $BaAl_4$-type compounds having such a non-stoichiometry. Accordingly, the non-stoichiometric $(La_{0.3}Ge_{0.7})(Ni_{0.85}Ge_{0.15})_2Ge_2$ metastable compound discovered in this study is interesting from the viewpoint of the crystal chemistry and stability of the $BaAl_4$-type structure.

It is interesting to compare the lattice parameters of the non-stoichiometric and stoichiometric compounds to discuss the crystal chemistry of the $BaAl_4$-type compounds because they contain the same kind of elements and just have different compositions. Compared to the lattice parameters of the stoichiometric $LaNi_2Ge_2$, $a = 4.1860(6)$ Å and $c = 9.902(1)$ Å [19], the non-stoichiometric $(La_{0.3}Ge_{0.7})(Ni_{0.85}Ge_{0.15})_2Ge_2$ has a shorter a-axis lattice parameter and longer c-axis lattice parameter. The ratio of lattice parameters c/a is much larger than that of the stoichiometric one, 2.366 [19]. The volume is also much larger than that of the stoichiometric one, 173.51 Å^3 [19]. This comparison is summarized in table 3. As mentioned above, since the 70% (La, Ge) site in the structure of the non-stoichiometric compound is occupied by the Ge atoms, of which the atomic radius is much smaller than that of La, it is easily expected that the lattice parameters of the non-stoichiometric compound become smaller than those of the stoichiometric one. Actually, the a-axis lattice parameter of the non-stoichiometric compound is slightly smaller. However, it should be noted that the c-axis parameter of the non-stoichiometric compound is much larger than that of the stoichiometric one. These comparisons between $(La_{0.3}Ge_{0.7})(Ni_{0.85}Ge_{0.15})_2Ge_2$ and $LaNi_2Ge_2$ indicate that the c-axis lattice parameter of the $BaAl_4$-type compound depends not only on the atomic radius of the Ba-site atom but also another factor, suggesting effects of the Ge atoms substituting to the Ni site on the c-axis parameter, although Ge (1.23 Å) has almost the same atomic radius as Ni (1.25 Å).

In order to discuss the c-axis lattice parameter in detail, the crystal structures of $(La_{0.3}Ge_{0.7})(Ni_{0.85}Ge_{0.15})_2Ge_2$ and $LaNi_2Ge_2$ should be compared in detail. The details of the crystal structure of $LaNi_2Ge_2$ have been already reported [19]. Important results of these two compounds in this study are listed in table 3. It should be noted that the interatomic Ge–Ge distance of $(La_{0.3}Ge_{0.7})(Ni_{0.85}Ge_{0.15})_2Ge_2$ is almost the same as that of $LaNi_2Ge_2$, although they have different c-axis lattice parameter. In addition, it should be noted that the interatomic

Table 3. Comparison of structural parameters between $(La_{0.3}Ge_{0.7})(Ni_{0.85}Ge_{0.15})_2Ge_2$ and $LaNi_2Ge_2$ [20]. z(Ge) means the z atomic position of the Ge site. TM and R mean atoms of the Al_a site and Ba site in the $BaAl_4$-type structure, respectively. L(X) where X = TM, Ge, R, means the atomic layer composed by the X atoms perpendicular to the c-axis in the tetragonal unit cell.

	$(La_{0.3}Ge_{0.7})(Ni_{0.85}Ge_{0.15})_2Ge_2$	$LaNi_2Ge_2$
Unit cell		
a (Å)	4.080 10(15)	4.1860(6)
c (Å)	10.677 90(49)	9.902(1)
c/a	2.6192	2.366
V (Å)	177.7573(122)	173.51
z(Ge)	0.374 51(15)	0.3667(2)
Interatomic distance		
Ge–TM (Å)	2.435	2.391
Ge–R (Å)	3.181[a]	3.241
Ge–Ge (Å)	2.676	2.640
TM–TM (Å)	2.884	2.960
Interlayer distance		
L(TM)–L(Ge) (Å)	1.329	1.153
L(Ge)–L(R) (Å)	1.338	1.320

[a] Interatomic distance of Ge–R of the $(La_{0.3}Ge_{0.7})(Ni_{0.85}Ge_{0.15})_2Ge_2$ is estimated using the ideal position of the R site atom because the atomic position of (La, Ge) of $(La_{0.3}Ge_{0.7})(Ni_{0.85}Ge_{0.15})_2Ge_2$ is not ideal.

Ge–TM distance (TM: atom at the original Ni site) of $(La_{0.3}Ge_{0.7})(Ni_{0.85}Ge_{0.15})_2Ge_2$ is much longer than that of $LaNi_2Ge_2$. In order to understand these differences, the interlayer distance between the two nearest layers perpendicular to the c-axis is calculated and also listed in table 3. It is found that the interlayer distance between Ge and $(Ni_{0.85}Ge_{0.15})$ layers of $(La_{0.3}Ge_{0.7})(Ni_{0.85}Ge_{0.15})_2Ge_2$ is much longer than that of $LaNi_2Ge_2$. On the other hand, the interlayer distance between Ge and Ge layers of $(La_{0.3}Ge_{0.7})(Ni_{0.85}Ge_{0.15})_2Ge_2$ which corresponds to the interatomic Ge–Ge distance is almost the same as that of $LaNi_2Ge_2$, as mentioned above. These comparisons are also shown in figure 11. This figure leads us to a clear important conclusion about the difference in the c-axis lattice parameter of these compounds. That is, the longer c-axis parameter of $(La_{0.3}Ge_{0.7})(Ni_{0.85}Ge_{0.15})_2Ge_2$ than that of $LaNi_2Ge_2$ is simply attributable to the longer interlayer distance between the Ge and (Ni, Ge) layers of the former compared with that of the Ge and Ni layers of the latter. In other words, the interlayer distance between the Ge layers of $(La_{0.3}Ge_{0.7})(Ni_{0.85}Ge_{0.15})_2Ge_2$ is hardly affected by a lot of substitution of Ge atoms to La sites.

3.3. Electronic properties of the non-stoichiometric $BaAl_4$-type $(La_{0.3}\ Ge_{0.7})(Ni_{0.85}Ge_{0.15})_2Ge_2$ compound

Figure 12 shows the temperature dependence of the thermoelectric power of the non-stoichiometric $BaAl_4$-type $(La_{0.3}Ge_{0.7})(Ni_{0.85}Ge_{0.15})_2Ge_2$ compound. Results from the amorphous $La_6Ni_{34}Ge_{60}$ alloy are also shown in the figure for comparison. It is found that the thermoelectric powers of both materials are negative and small, and they show only slight temperature dependence in the measured temperature range. These behaviours indicate that they are simple metals. It should be noted that both results are almost the same as each other although the amorphous alloy has slightly larger negative values. Since the thermoelectric power is proportional to the derivative of the logarithm of the density of states at the Fermi level, the thermoelectric power is directly related to the electronic structure, i.e. the density

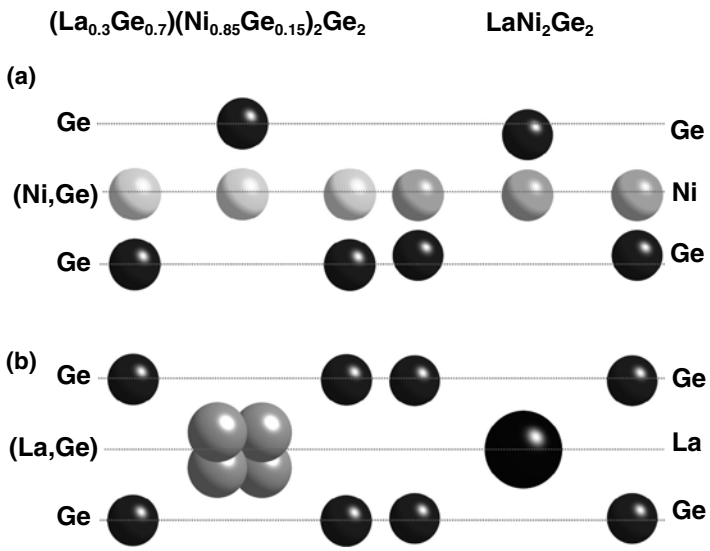

Figure 11. Comparison of interlayer distance perpendicular to the *c*-axis between $(La_{0.3}Ge_{0.7})(Ni_{0.85}Ge_{0.15})_2Ge_2$ and $LaNi_2Ge_2$. (a) Ge–(Ni, Ge)–Ge layers, (b) Ge–(La, Ge)–Ge layers.

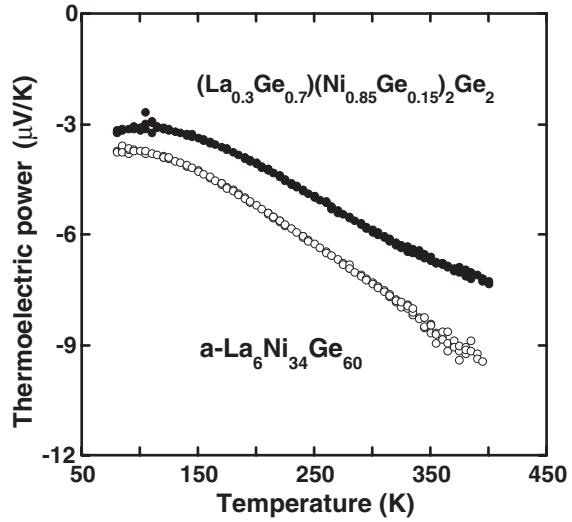

Figure 12. The temperature dependence of the thermoelectric power of the non-stoichiometric $BaAl_4$-type $(La_{0.3}Ge_{0.7})(Ni_{0.85}Ge_{0.15})_2Ge_2$ and the amorphous $La_6Ni_{34}Ge_{60}$.

of states itself at the Fermi level and its slope at the Fermi level. Accordingly, these results indicate that electronic structures around the Fermi level of the $(La_{0.3}Ge_{0.7})(Ni_{0.85}Ge_{0.15})_2Ge_2$ compound and amorphous $La_6Ni_{34}Ge_{60}$ alloy are similar to each other.

Figure 13 shows the temperature dependence of the electrical resistivity of the non-stoichiometric $BaAl_4$-type $(La_{0.3}Ge_{0.7})(Ni_{0.85}Ge_{0.15})_2Ge_2$ compound. The electrical resistivities are normalized by the value at 293 K. Results from the amorphous $La_6Ni_{34}Ge_{60}$ alloy are also shown in the figure for comparison. It is found that the electrical resistivity of the

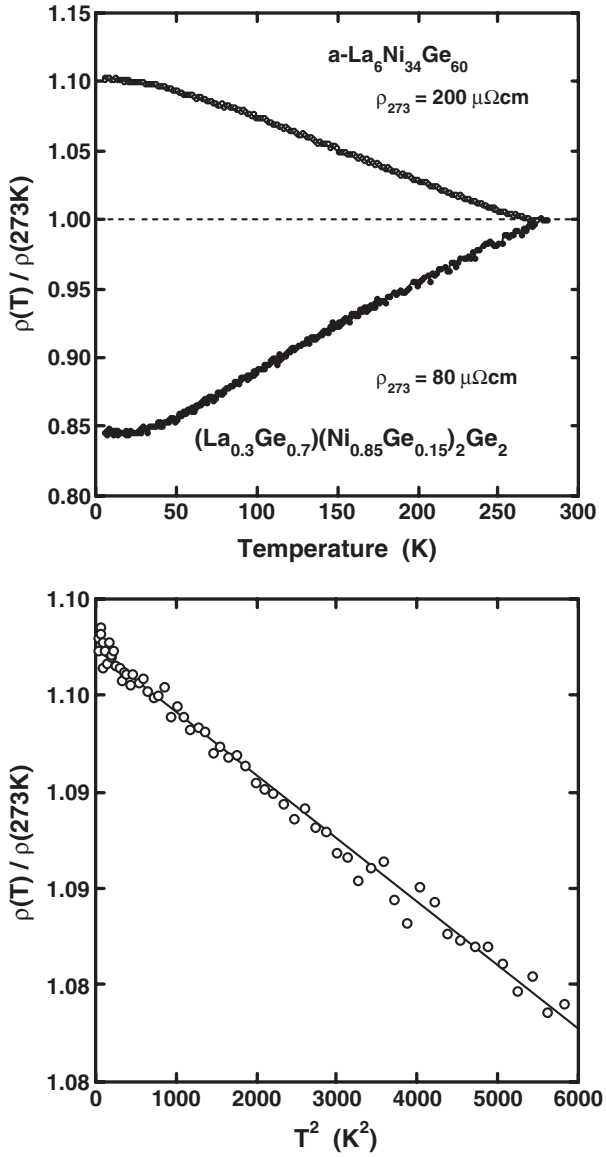

Figure 13. (a) The temperature dependence of the electrical resistivity of the non-stoichiometric $BaAl_4$-type $(La_{0.3}Ge_{0.7})(Ni_{0.85}Ge_{0.15})_2Ge_2$ and the amorphous $La_6Ni_{34}Ge_{60}$. The electrical resistivities are normalized by the value at 293 K. (b) The quadratic temperature dependence of the amorphous $La_6Ni_{34}Ge_{60}$ below about 77 K. The solid line indicates a fitting result using a quadratic temperature dependence.

compound decreases with decreasing temperature and then almost saturates around 20 K. This temperature dependence indicates that this compound is metallic although it is highly Ge-rich. However, it is found that the temperature dependence is small; the ratio $\rho(5\ \mathrm{K})/\rho(273\ \mathrm{K})$ is about 0.85. Besides, the electrical resistivity of the compound at 293 K is about 80 $\mu\Omega$ cm. These are attributable to the fine grains, about 500 nm in diameter, as shown in figure 4.

In terms of the temperature dependence of the electrical resistivity of the amorphous $La_6Ni_{34}Ge_{60}$ alloy, the resistivity increases linearly with decreasing temperature at high

temperatures and then shows quadratic temperature dependence at low temperatures, as shown in figure 12(b). This is a typical temperature dependence of non-magnetic amorphous alloys having high electrical resistivity above 100 $\mu\Omega$ cm, as pointed out by Mizutani [20]. In his reports, he called this type of temperature dependence of electrical resistivity 'type C' of 'group V amorphous alloys', of which the Fermi level lies in the sp-band of the electronic structure, i.e., sp-electrons mainly contribute to electrical conduction. Therefore, the electronic structure around the Fermi level of the amorphous $La_6Ni_{34}Ge_{60}$ alloy is dominated by the sp-band. As mentioned above, since the electronic structures around the Fermi level of the $(La_{0.3}Ge_{0.7})(Ni_{0.85}Ge_{0.15})_2Ge_2$ compound and amorphous $La_6Ni_{34}Ge_{60}$ alloy are similar to each other, sp-electrons also mainly contribute to the electrical conduction of the $(La_{0.3}Ge_{0.7})(Ni_{0.85}Ge_{0.15})_2Ge_2$ compound. This is consistent with the results of thermoelectric power in figure 12 because they are small and have slight temperature dependence.

The band calculations of the electronic structure of the $LaNi_2Ge_2$ compound have been reported, and they show that its electronic structure around the Fermi level is dominated by the Ni 3d-band [21]. This is different from the electronic structure around the Fermi level of the $(La_{0.3}Ge_{0.7})(Ni_{0.85}Ge_{0.15})_2Ge_2$ compound, which is mainly dominated by the sp-band, as discussed above. This means that the Ni 3d-band in the $(La_{0.3}Ge_{0.7})(Ni_{0.85}Ge_{0.15})_2Ge_2$ compound is fully occupied and that its Fermi level is located in the sp-band above the Ni 3d-band. The band calculations have also shown that the La 4f-band is located in a much higher energy region than the Ni 3d-band [21]. This indicates that there is a pseudogap between the Ni 3d- and La 4f-bands which has a low density of sp-states. Accordingly, the Fermi level of the $(La_{0.3}Ge_{0.7})(Ni_{0.85}Ge_{0.15})_2Ge_2$ compound is located at the pseudogap. This condition is attributable to the metastability of $(La_{0.3}Ge_{0.7})(Ni_{0.85}Ge_{0.15})_2Ge_2$ because a pseudogap contributes most efficiently to lowering the electronic energy of the system concerned and stabilizes the system. The important role of the pseudogap at the Fermi level in the electronic structure on the phase stability of the s–p bonded $BaAl_4$-type AX_4 compounds has been also reported [10]. In those cases, the pseudogap separating X bonding from antibonding electronic states is effective for their phase stability. Although the origin of the formation of the pseudogap at the Fermi level among them is not found, it can be concluded that the $BaAl_4$-type compounds are stabilized by lowering the electronic energy of the system concerned due to the pseudogap at the Fermi level in the electronic structure.

4. Conclusions

Both the crystallization of the Ge-rich amorphous $La_6Ni_{34}Ge_{60}$ alloy and the crystallized metastable compound have been investigated. It is found that the $La_6Ni_{34}Ge_{60}$ amorphous alloy shows a polymorphic transformation to a metastable compound on crystallizing. The metastable compound is identified to be of the $BaAl_4$-type ($ThCr_2Si_2$-type) structure by SEM-EPMA, x-ray powder diffraction and the Rietveld analysis, and HRTEM and image simulation. It is found that the Ba and Al_a sites of the $BaAl_4$-type structure in the metastable compound are also occupied by Ge atoms. The determined formula of the metastable compound is $(La_{0.3}Ge_{0.7})(Ni_{0.85}Ge_{0.15})_2Ge_2$. It should be noted that this is a new highly non-stoichiometric $BaAl_4$-type compound in the La–Ni–Ge system. The atomic position of the (La, Ge) site in $(La_{0.3}Ge_{0.7})(Ni_{0.85}Ge_{0.15})_2Ge_2$ is analysed to be non-ideal.

The unit cell parameters of $(La_{0.3}Ge_{0.7})(Ni_{0.85}Ge_{0.15})_2Ge_2$ are calculated to be $a = 4.080\,10(15)$ Å, $c = 10.677\,90(49)$ Å, respectively. They are shorter and longer than those of the stoichiometric $LaNi_2Ge_2$, respectively. The ratio of lattice parameters c/a and the unit cell volume of $(La_{0.3}Ge_{0.7})(Ni_{0.85}Ge_{0.15})_2Ge_2$ are 2.6192 and about 177.7513(122) Å^3, respectively. These values are much larger than those of $LaNi_2Ge_2$.

It is found that the interlayer distances between the La site and Ge site layers of these compounds are almost the same as each other. On the other hand, those of the Ge site and Ni site layers of $(La_{0.3}Ge_{0.7})(Ni_{0.85}Ge_{0.15})_2Ge_2$ are much longer than those of $LaNi_2Ge_2$. These indicate that the longer *c*-axis lattice parameter of $(La_{0.3}Ge_{0.7})(Ni_{0.85}Ge_{0.15})_2Ge_2$ is attributable only to the longer interlayer distance between the original Ge site and the original Ni site layers.

The temperature dependence of the thermoelectric power of the non-stoichiometric $BaAl_4$-type $(La_{0.3}Ge_{0.7})(Ni_{0.85}Ge_{0.15})_2Ge_2$ compound and amorphous $La_6Ni_{34}Ge_{60}$ alloy are clarified. It should be noted that both results are almost the same as each other, indicating that the electronic structures around the Fermi level of these materials are similar to each other. Their temperature dependence of the electrical resistivity is also investigated. Considering the result of their thermoelectric powers and the temperature dependence of the electrical resistivity of the amorphous alloy, it is concluded that the sp-band contributes to the electronic structure around the Fermi level of the $(La_{0.3}Ge_{0.7})(Ni_{0.85}Ge_{0.15})_2Ge_2$ compound. In addition, it is also noted that the Fermi level of the $(La_{0.3}Ge_{0.7})(Ni_{0.85}Ge_{0.15})_2Ge_2$ compound is located at the pseudogap. This condition is attributable to the metastability of $(La_{0.3}Ge_{0.7})(Ni_{0.85}Ge_{0.15})_2Ge_2$ because the pseudogap contributes most efficiently to lowering the electronic energy of the system concerned and stabilizes the system.

Acknowledgments

The authors are grateful for Y Syono (IMR, Tohoku University) for his useful discussion. They are also grateful for T Nojima (CLTS, Tohoku University) for his support of the electrical resistivity measurement. This research was partially supported by the Ministry of Education, Science, Sports and Culture, Grant-in-Aid for Scientific Research on Priority Areas.

References

[1] Imafuku M, Sato S, Koshiba H, Matsubara E and Inoue A 2000 *Mater. Trans.* **41** 1526
[2] Louzguine D V, Takeuchi A and Inoue A 2001 *J. Non-Cryst. Solids* **289** 196
[3] Izumi F and Ikeda T 2000 *Mater. Sci. Forum* **321–324** 198
[4] Dorrscheidt W, Niess N and Schafer H 1976 *Z. Naturf.* b **31** 890
[5] Rieger W and Parthe E 1969 *Monatsh. Chem.* **100** 444
[6] Andress K R and Alberti E 1935 *Z. Metallk.* **27** 126
[7] Villars P and Calvert L D (ed) 1991 *Pearson's Handbook of Crystallographic Data for Intermetallic Phases* 2nd edn, vol 1 (Metals Park, OH: ASM International) p 670
[8] Villars P and Calvert L D (ed) 1991 *Pearson's Handbook of Crystallographic Data for Intermetallic Phases* 2nd edn, vol 1 (Metals Park, OH: ASM International) pp 129–31
[9] Pearson W B 1985 *J. Solid State Chem.* **56** 278
[10] Haussermann U, Amerioun S, Eriksson L, Lee C S and Miller G J 2002 *J. Am. Chem. Soc.* **124** 4371
[11] Welter R, Venturini G, Malaman B and Ressouche E 1993 *J. Alloys Compounds* **202** 165
[12] Miller G J, Li F and Franzen H F 1993 *J. Am. Chem. Soc.* **115** 3739
[13] Just G and Paufler P 1996 *J. Alloys Compounds* **232** 1
[14] Gustenau E, Herzig P and Neckel A 1997 *J. Alloys Compounds* **262** 516
[15] Biehl E and Deiseroth H J 1999 *Z. Anorg. Allg. Chem.* **625** 389
[16] Seo D K and Corbett J D 2000 *J. Am. Chem. Soc.* **122** 9621
[17] von Schnering H G, Turck R, Honle W, Peters K, Peters E M, Kremer R and Chang J H 2002 *Z. Anorg. Allg. Chem.* **6288** 2772
[18] Grytsiv A, Kaczorowski D, Leithe-Jasper A, Rogl P, Godart C, Potel M and Noel H 2002 *J. Solid State Chem.* **163** 37
[19] Venturini G and Malaman B 1996 *J. Alloys Compounds* **235** 201
[20] Mizutani U, Sato K, Sakamoto I and Yonemitsu K 1995 *J. Phys. F: Met. Phys.* **18** 1995
Mizutani U 2001 *Introduction to the Electron Theory of Metals* (Cambridge: Cambridge University Press) p 481
[21] Yamagami H 1999 *J. Phys. Soc. Japan* **68** 1975